A New Approach to HVDC System Control for Damping SSO Using the Novel Eigenvalue Analysis Program

Dong-Joon Kim†, Hae-Kon Nam* and Young-Hwan Moon**

Abstract - This paper presents a new approach to HVDC system control for damping subsynchronous oscillation (SSO) involving HVDC converters and turbine generator shaft systems. This requires a novel eigenvalue analysis (NEA) program, derivation of HVDC system modeling considering steady-state conditions and dynamic conditions in the combined AC/DC system, and an appropriate control scheme. The method suggested makes possible the design of a subsynchronous oscillation damping controller (SODC) to provide positive damping torque for the range of torsional modes in combined AC/DC systems. There are three steps involved in the design of a SODC; first the worst torsional mode is determined using the NEA program, next the SODC parameters are designed for the range of that torsional mode, and then finally an off-line simultaneous time domain program such as PSCAD/EMTDC is used to verify the parameters of the SODC. The suggested SODC design method is applied to two AC/DC systems, and its practicality is verified using the PSCAD/EMTDC simulation program.

Keywords: Damping Controller, Eigenvalue analysis, HVDC system, Subsynchronous Oscillation

1. Introduction

In 1977, tests on the High Voltage Direct Current system (HVDC) at Square Butte, which consists of a ±250 kV, 500 MW DC link and a 435 MW turbine generator, showed that the HVDC system was destabilizing the first torsional mode of vibration at 11.5 Hz when one AC transmission line was switched out [1]. Since then, subsynchronous torsional oscillations, due to the interaction between the turbine generator units and the HVDC system, have become a significant matter of concern in AC/DC operation and planning. The phenomenon has led to questioning the concept of whether a series capacitor compensated transmission system is necessary to cause subsynchronous torsional oscillation of the shafts of turbine generator units.

Interaction between high-speed power controllers, such as HVDC converters, Static Var Compensation (SVC) systems, and Power System Stabilizers (PSS), and turbine generators has led to an understanding of the wide range of possible turbine generator shaft reactions. These have been broadly represented by the term subsynchronous oscillation (SSO) [2-3]. Since SSO does not have a resonance property, which implies a periodic phenomenon and two oscillators, it is distinguished from subsynchronous resonance.

The SSO arising in the HVDC and turbine generator shaft system is inherently based on the current control loop of the rectifier converter to maintain constant current or power [4]. Since turbine generator torsional modes have very little inherent damping, shaft oscillations are sustained for a considerable time after they are stimulated. Cumulative damage to the shaft as a result of fatigue can lead to reduced life and fatigue failure. It has been shown that DC current control at the rectifier will produce negative damping of rotor oscillations over some frequency range. Hence, current control of HVDC systems contributes a component of negative damping to shaft oscillation. Therefore, a supplementary damping controller needs to be incorporated into the current control loop of the rectifier to compensate for the negative electrical damping caused predominantly by the current control loop.

HVDC systems possess sufficiently rapid power control capabilities such that the supplementary subsynchronous oscillation damping controller in the HVDC system can provide positive damping over subsynchronous frequencies in the range 5 to 55 Hz. The effectiveness of HVDC systems to provide damping torque at higher frequencies depends on the design of the HVDC auxiliary controller and the choice of the parameters. The auxiliary Subsynchronous Oscillation Damping Controller (SODC) should be tuned with great care to avoid additional negative damping for such frequencies. An appropriate control strategy is required.

Because of the complexity of AC and HVDC system

The Transactions of the KIEE, Vol.53A, No.3, MAR. 2004, pp.140-151 : A paper recommended and approved by the Editorial Board of the KIEE Power Engineering Society for translation for the KIEE International Transaction on PE.

† Corresponding Author: Dept. of Electrical Engineering, Chonnam National University, Korea. (djkim0419@keri.re.kr)

* Dept. of Electrical Engineering, Chonnam National University, Korea. (hknam@chonnam.ac.kr)

** Electricity Market Technology Research Group, KERI, Korea. (yhmoon@keri.re.kr)

Received May 19, 2003 ; Accepted December 27, 2003

Because of the complexity of AC and HVDC system modeling for the study of subsynchronous oscillation, few studies have been reported regarding the design of the SODC in HVDC systems. It is necessary to use a small-signal stability analysis program in designing the SODC, which takes into account the dynamics of the network as well as the dynamics of the machine multi-mass shaft systems and the HVDC system. In addition, a simultaneous time domain three-phase simulation program or an electrical scale-model analog simulator is required in order to verify the feasibility of the designed control parameters.

The auxiliary SODC in the HVDC system was first reported in reference [4]. It was given the acronym SSDC, and utilized the frequency of the commutation bus as its input signal. The compensated bus frequency is derived from measurement of the AC commutation bus voltage and current, using these for compensating the line drop. The design procedure for the SSDC depends on a small-signal stability program and a scaled down analog simulator. This small-signal stability program indirectly constructs the linear system state matrix from the nonlinear time-domain program through numerical differentiation. Hence, it is susceptible to inaccuracy. The procedure uses the small-signal stability program to calculate the frequency response of the electrical damping component in phase with the rotor speed. Such a procedure is effective for tuning the control parameters for phase compensation. However, since this method separates the electrical system from the mechanical system, modes including both the mechanical system and the electrical system could not be considered simultaneously. In addition, the synthesized voltage frequency from the AC voltage at the commutating bus is insensitive to swings when measured at a distance from the generators and has less observability when the load on the DC link is increased.

The novel eigenvalue analysis (NEA) program used in this paper involves a steady-state power flow module for initializing states, and a dynamic module capable of constructing the system matrix in which the HF machine model, the 6-mass shaft system model, and the HVDC dynamic model, are included to analyze the AC/DC subsynchronous oscillation. The derived HF linear machine model includes two additional state equations, representing the dynamics of the stator, to those included in the conventional stability program. The dynamic modeling of the HVDC system consists of a converter model, a DC line dynamic model, and a current control model.

This paper suggests an effective method for designing a SODC for damping SSO in AC/DC systems. The suggested design method uses three steps as follows: 1) from the NEA program the most unstable torsional mode is identified for the purpose of designing the SODC, 2) the time constants of the SODC are then tuned to compensate the phase lag due to the current controller and the AC/DC networks using the frequency response and eigenvalue analysis, and 3) the designed SODC is verified using the commercial Electro-magnetic Transient including Direct Current Program (EMTDC). The method is verified by application to a single HVDC radial system and a HVDC system in parallel with an AC transmission system.

2. The NEA Program and Modeling of HVDC Systems

The NEA program [21-22] can investigate a wide range of HF small-signal stability of multi-machine power systems, such as SSR and SSO, as a result of the interaction between a turbine-generator and either a HVDC converter, SVC or PSS. The modeling of a HVDC system includes steady-state modeling for power flow studies and dynamic modeling for eigenvalue analysis.

2.1 The NEA Program

The NEA program uses a novel approach for constructing the state matrix of the multiple machine power system using linear equations for each device in its own frame. The complete set of state matrixes is derived simply by transforming the output equations of both the machine and the network into the reference frame of the other. The flexibility of modular construction [6, 7, 10 and 11] adopted in the NEA program allows modeling of a wide variety of power system components interconnected by an electrical transmission network, and makes the computer implementation of adding/modifying component models much easier. Additional explanation about the NEA program will be omitted.

2.2 Steady-State Modeling of HVDC Systems

The switching response of the converter is so fast that it is usual to model it by algebraic equations. The HVDC transmission model includes a converter transformer with load tap changer, bridge, and DC line. In steady state operation, the inverter transformer is controlled automatically to optimize the HVDC voltage and the rectifier transformer load tap changer is controlled to hold the firing angle at its nominal value. The following assumptions are used in the converter equations (A.1-A.4) [25].

- The direct current has no ripple.
- The AC systems at the rectifier and inverter have pure sinusoidal, constant frequency, and balanced voltage sources behind balanced impedances.
- The converter transformers do not saturate.

2.3 Dynamic Modeling of HVDC Systems

In this paper, the dynamic equations of converter bridge circuits are represented by steady state equations used in the power flow model due to the almost instantaneous response of the thyristor converter [4]. In addition, the state matrix of the HVDC control is constructed by assuming that the HVDC system operates in normal conditions, in which the PI controller in the rectifier controls the DC current while the controller in the inverter maintains the constant extinction angle, γ.

2.3.1 Dynamic Modeling of the DC Line and Its Control

The HVDC line is modeled as a "T" line model, as shown in Fig. 1. A DC line consists of a smoothing reactor, line resistance, harmonic filter, and shunt line capacitor. The dynamic equations for the converters are the same algebraic equations used in power-flow calculations because of the fast switching response of converters.

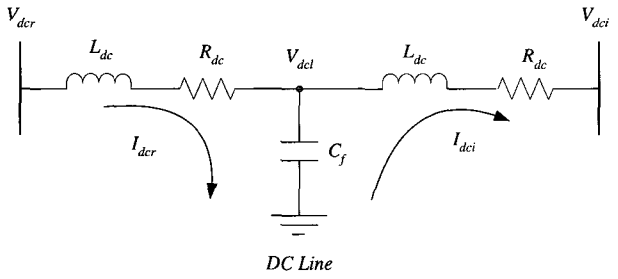

Fig. 1 HVDC Transmission "T" Line Model

In this paper, the PI current controller is modeled for current control of the rectifier, as demonstrated in Fig. 2. Furthermore, the PI current controller is assumed to have a Phase Lock Loop (PLL) circuit to synchronize with the power system. The advantage of using a PLL control is greater stability of operation than is achieved with the other control schemes, in which the HVDC links are operated with weak AC systems. The phase lag resulting from the PLL circuit is represented as α_ϕ, as presented in Fig. 2; it can be modeled as a washout filter with a time constant of approximately 0.04 seconds.

The control mode of the inverter is usually constant extinction angle (CEA) control. Therefore, this paper does not model the controller of the inverter in detail. In terms of torsional oscillation, the worst control mode for HVDC systems is the constant current mode, or constant real power control of the rectifier. The rectifier is operated as a constant current load or constant power. Such loading conditions decrease the damping of the subsynchronous oscillations. For this reason, it is sufficient only to consider modeling the current control of the rectifier to design a torsional damping controller.

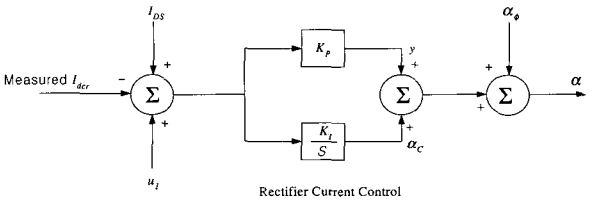

Fig. 2 Constant Current Control of the Rectifier

$$\alpha = \alpha_C + \alpha_\phi + y \tag{1}$$

$$\alpha = (I_{ds} - I_{dcr} + u_1)K_p + (I_{ds} - I_{dcr} + u_1)\frac{K_I}{s} + \alpha_\phi \tag{2}$$

$$\alpha_\phi = -\phi_{PLL} + \theta_{E_{ACR}} = \frac{T_p s}{1 + T_p s}\theta_{E_{ACR}} \tag{3}$$

2.3.2 Linearization of HVDC Systems

Using the dynamic equations of the HVDC system above the linearized equation of the DC line at the rectifier is:

$$L_{dc} p\Delta I_{dcr} = \Delta V_{dcl} - k_1 \Delta E_{acr} - k_2 \Delta\alpha + (-k_3 - R_{dc})\Delta I_{dcr} \tag{4}$$

where,

$$k_1 = N_r \frac{3\sqrt{2}}{\pi}\cos\alpha_0$$

$$k_2 = -N_r \frac{3\sqrt{2}}{\pi} E_{acr0}\sin\alpha_0$$

$$k_3 = -N_r \frac{3X_{cr}}{\pi} - 2N_r R_{cr}$$

$$k_4 = -N_r L_{ci}$$

The linear forms of the current controller at the rectifier are:

$$\Delta\alpha = \Delta\alpha_C + \Delta y + \Delta\alpha_\phi = \Delta\alpha_C + \Delta y - \Delta\phi_{PLL} + \Delta\theta_{E_{ACR}} \tag{5}$$

$$\Delta\alpha_C = -\frac{K_I}{s}\Delta I_{dcr} + \frac{K_I}{s}\Delta u_1 \tag{6}$$

$$\Delta y = -K_p \Delta I_{dcr} + K_p \Delta u \tag{7}$$

The linearized equations of the PLL circuit are:

$$\Delta\alpha_\phi = -\Delta\phi_{PLL} + \Delta\theta_{E_{ACR}} = \frac{T_p s}{1 + T_p s}\Delta\theta_{E_{ACR}} \tag{8}$$

$$\Delta\phi_{PLL} = \frac{1}{1+T_p s}\Delta\theta_{E_{ACR}} \tag{9}$$

$$T_p p\Delta\phi_{PLL} = -\Delta\phi_{PLL} + \Delta\theta_{E_{ACR}} \tag{10}$$

The linearized equations of the rectifier can be expressed as:

$$\begin{bmatrix} L_{dc} & 0 & 0 \\ 0 & 1 & 0 \\ 0 & 0 & T_p \end{bmatrix} p \begin{bmatrix} \Delta I_{dcr} \\ \Delta\alpha_c \\ \Delta\phi_{PLL} \end{bmatrix} = \begin{bmatrix} (k_3 - R_{dcr} - K_p k_2) & k_2 & -k_2 \\ -K_I & 0 & 0 \\ 0 & 0 & -1 \end{bmatrix} \begin{bmatrix} \Delta I_{dcr} \\ \Delta\alpha_c \\ \Delta\phi_{PLL} \end{bmatrix} + \begin{bmatrix} -1 \\ 0 \\ 0 \end{bmatrix} \Delta V_{dcrI} \tag{11}$$
$$+ \begin{bmatrix} k_2 & k_1 \\ 0 & 0 \\ 1 & 0 \end{bmatrix} \begin{bmatrix} \Delta\theta_{E_{acr}} \\ \Delta E_{acr} \end{bmatrix}$$

It is assumed that the control mode of the inverter is constant extinction control mode. Therefore, the inverter control can be ignored. The inverter linearized equations are:

$$L_{dc} p\Delta I_{dci} = -(k_5\Delta E_{aci} + k_6\Delta\gamma + k_7\Delta I_{dci}) + \Delta V_{dcl} - R_{dc}\Delta I_{dci} \tag{12}$$

where,

$$k_5 = N_i \frac{3\sqrt{2}}{\pi}\cos\gamma_0$$

$$k_6 = -N_i \frac{3\sqrt{2}}{\pi} E_{aci0}\sin r_0$$

$$k_7 = -N_i\left(\frac{3\sqrt{2}}{\pi} - 2R_{cr}\right)$$

The DC Line linearized equation is:

$$C_l p\Delta V_{dcl} = \Delta I_{dcr} - \Delta I_{dci} \tag{13}$$

Therefore, the HVDC system is modeled by a fifth-order differential equation and the matrix form can be constructed as:

$$\begin{bmatrix} L_{dc} & 0 & 0 & 0 & 0 \\ 0 & 1 & 0 & 0 & 0 \\ 0 & 0 & T_p & 0 & 0 \\ 0 & 0 & 0 & L_{dc} & 0 \\ 0 & 0 & 0 & 0 & C_l \end{bmatrix} p \begin{bmatrix} \Delta I_{dcr} \\ \Delta\alpha_c \\ \Delta\phi_{PLL} \\ \Delta I_{dci} \\ \Delta V_{dcl} \end{bmatrix} = \begin{bmatrix} (k_3 - K_p k_2 - R_{dc}) & k_2 & -k_2 & 0 & -1 \\ -K_I & 0 & 0 & 0 & 0 \\ 0 & 0 & -1 & 0 & 0 \\ 0 & 0 & 0 & (-k_7 - R_{dc}) & 1 \\ 1 & 0 & 0 & -1 & 0 \end{bmatrix} \begin{bmatrix} \Delta I_{dcr} \\ \Delta\alpha_c \\ \Delta\phi_{PLL} \\ \Delta I_{dci} \\ \Delta V_{dcl} \end{bmatrix} +$$
$$\begin{bmatrix} k_2 & k_1 & 0 & 0 \\ 0 & 0 & 0 & 0 \\ 1 & 0 & 0 & 0 \\ 0 & 0 & 0 & -k_5 \\ 0 & 0 & 0 & 0 \end{bmatrix} \begin{bmatrix} \Delta\theta_{acr} \\ \Delta E_{acr} \\ \Delta\theta_{aci} \\ \Delta E_{aci} \end{bmatrix} \tag{14}$$

2.3.3 AC/DC Interfacing

For the analysis of SSO, including the interaction between the HVDC and AC systems, it is necessary that the HVDC dynamic model be interfaced with the AC system containing network dynamics as well as device dynamics, such as machines and torsional systems. Using AC current and voltage, the AC/DC interface is modeled. The AC current is derived by manipulating the HVDC equations, and is used as input to AC dynamic equations. The AC voltage, in polar coordinates, is used as the input to the HVDC systems.

From the converter and controller equations described in the Appendix, rectangular AC current in the rectifier can be derived using equation (A.1) as:

$$\cos\theta_r = \cos\alpha - \frac{X_{cr} I_{dc}}{\sqrt{2}E_{acr}} \tag{15}$$

$$\theta_r = \theta_{E_{acr}} - \theta_{I_{acr}} \tag{16}$$

$$\begin{bmatrix} \Delta\theta_{I_{acr}} \\ \Delta I_{acr} \end{bmatrix} = \begin{bmatrix} \left(-\frac{1}{\sin\theta_r}\frac{X_{cr}}{\sqrt{2}E_{acr}} + K_p\frac{\sin\alpha}{\sin\theta_r}\right) & -\frac{\sin\alpha}{\sin\theta_r} & \frac{\sin\alpha}{\sin\theta_r} & -K_p\frac{\sin\alpha}{\sin\theta_r} \\ \frac{\sqrt{6}}{\pi}N_i T & 0 & 0 & 0 \end{bmatrix} \begin{bmatrix} \Delta I_{dcr} \\ \Delta\alpha \\ \Delta\phi_{PLL} \\ \Delta u \end{bmatrix}$$
$$+ \begin{bmatrix} 1 - \frac{\sin\alpha}{\sin\theta_r} & -\frac{1}{\sin\theta_r}\frac{X_{cr} I_{dcr}}{\sqrt{2}E_{acr}^2} \\ 0 & 0 \end{bmatrix} \begin{bmatrix} \Delta\theta_{E_{acr}} \\ \Delta E_{acr} \end{bmatrix} \tag{17}$$

The relationship between the polar form, in which HVDC systems are modeled, and the rectangular form, which is used in the AC network equations, is

$$\begin{bmatrix} \Delta I_{acrR} \\ \Delta I_{acrI} \end{bmatrix} = \begin{bmatrix} -I_{acr}\sin\theta_{I_{acr}} & \cos\theta_{I_{acr}} \\ I_{acr}\cos\theta_{I_{acr}} & \sin\theta_{I_{acr}} \end{bmatrix} \begin{bmatrix} \Delta\theta_{I_{acr}} \\ \Delta I_{acr} \end{bmatrix} \tag{18}$$

$$\begin{bmatrix} \Delta E_{acrR} \\ \Delta E_{acrI} \end{bmatrix} = \begin{bmatrix} -E_{acr}\sin\theta_{E_{acr}} & \cos\theta_{E_{acr}} \\ E_{acr}\cos\theta_{E_{acr}} & \sin\theta_{E_{acr}} \end{bmatrix} \begin{bmatrix} \Delta\theta_{E_{acr}} \\ \Delta E_{acr} \end{bmatrix} \tag{19}$$

In the inverter, using the converter equation the AC current is derived as:

$$\begin{bmatrix} \Delta\theta_{I_{aci}} \\ \Delta I_{aci} \end{bmatrix} = \begin{bmatrix} -\frac{1}{\sin\theta_i}\frac{X_{ci}}{\sqrt{2}E_{aci}} \\ \frac{\sqrt{6}}{\pi}N_i T \end{bmatrix} \Delta I_{dci} + \begin{bmatrix} 1 & -\frac{1}{\sin\theta_i}\frac{X_{ci} I_{dci}}{\sqrt{2}E_{aci}^2} \\ 0 & 0 \end{bmatrix} \begin{bmatrix} \Delta\theta_{E_{aci}} \\ \Delta E_{aci} \end{bmatrix} \tag{20}$$

3. Design Procedure of the SODC

Most damping problems occur on the rectifier side because the loading of the HVDC system appears as a

constant load on the rectifier side but as constant generation on the inverter side. In this paper, the design procedure for a supplementary subsynchronous oscillation damping controller in an HVDC control system is shown in Fig. 3.

There are three steps to design the supplementary SODC; the first step is to determine the worst torsional mode of several torsional modes using the NEA program. Then, the parameters of the supplementary damping controller are designed for the range of the determined torsional mode using the frequency response of the supplementary controller. In addition, the eigenvalues of the HVDC system, including the supplementary subsynchronous oscillation damping controller, are checked with the eigenvalue program. Finally, off-line time domain simulation, such as EMTP, is used to verify the parameters of the controller. If the degree of damping is not satisfied, proceed to step 2. Repeat until satisfactory results are obtained.

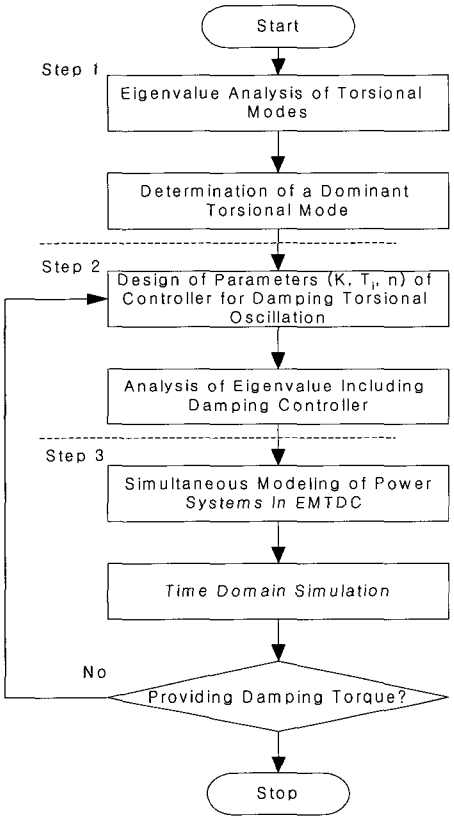

Fig. 3 Design Procedure of SODC

3.1 Eigenvalue Analysis: Step 1

The first step in design of the SODC is to analyze the interaction between the HVDC system and turbine-generator torsional system using the NEA program. Eigen analysis makes it possible to determine the overall system stabilities, including the HVDC system and the AC system. The real parts of the eigenvalue explain the stability of each mode. The least stable modes in the AC and DC systems are those of the torsional modes and the system mode. The system modes occur in the frequency range close to 1.0 Hz. Torsional modes have a wide range of frequency from 10 Hz to 50 Hz.

In designing the SODC, it is necessary to choose a dominant torsional mode when the loading conditions are considered. The highest loading in HVDC systems is the worst operating condition for the combined AC/DC system In this condition, the least stable mode becomes unstable so that this mode can be easily identified. Usually, this mode has lowest torsional frequency within a range of 7–15 Hz. The damping torque in the range of these frequencies is greatly affected by the electrical loading conditions.

3.2 Controller Design Procedure: Step 2

Negative electrical damping is inherently caused by the current control on the rectifier side. However, the current control is necessary for stable operation of the AC/DC systems. Adding the SODC to the HVDC current control loop can enhance the positive electrical damping of the torsional modes. Fig. 4 shows a block diagram of the transfer function from adjacent generator rotor speed to electrical torque, including a SODC. The input of the SODC is assumed to be a rotor speed signal, and the output of the SODC is a current reference signal. The advantage of this scheme is that there is no need for another transfer path between rotor speed and SODC, and also that no new inner current loop is created by the SODC.

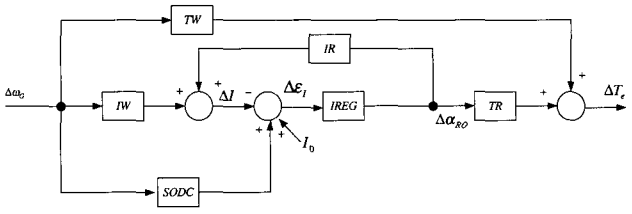

Fig. 4 Speed–Torque Transfer Path with the SODC

The explanations of transfer paths presented in Fig. 4 are

$$IW = \left.\frac{\partial I}{\partial \omega_G}\right|_{\Delta\alpha_{R0}=0} \tag{21}$$

$$IR = \left.\frac{\partial I}{\partial \Delta\alpha_{R0}}\right|_{\Delta\omega_{G0}=0} \tag{22}$$

$$TW = \left.\frac{\partial T_e}{\partial \omega_G}\right|_{\Delta\alpha_{R0}=0} \tag{23}$$

$$TR = \left.\frac{\partial T_e}{\partial \alpha_{R0}}\right|_{\Delta\omega_G=0} \tag{24}$$

where, ω_G = Generator Shaft Speed, $SODC$ = Subsynchronous Oscillation Damping Controller, T_e = Electrical Torque, I = DC Current.

It is convenient to isolate the SODC from other transfer paths as indicated in Fig. 5. There are three paths that contribute electrical damping torque. One path, *TW*, does not contain the current control path, and the remaining paths include the current control path, *ICLOSE*. Usually, the two paths shown in Fig. 5 provide negative electrical damping torque in AC/DC unified systems. The upper path, TW, accounts for electrical damping torque due to the AC transmission system as well as the inherent load characteristic independent of the HVDC control action. In the middle path shown in Fig. 5, the variation of rotor speed leads to an interaction with the HVDC control action. The main mechanism of the middle path is caused by a change in firing angle due to a shift in the phase of the AC network following a change in generator angle. This mechanism accounts for the primary influence over the interaction below 15-20 Hz.

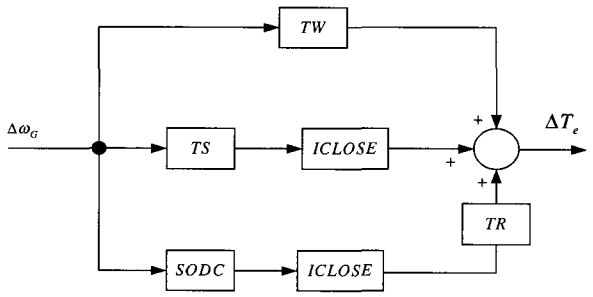

Fig. 5 Isolation of the SODC Path

The explanations of transfer paths shown in Fig. 5 are

$$TS = \text{System Characteristic Transfer Function} = -(IW)(TR) \tag{25}$$

$$ICLOSE = \text{Closed Loop Current Control Transfer Function} = \frac{(IREG)(IR)}{1+(IREG)(IR)} \tag{26}$$

The basic concept of synthesizing a SODC is to provide electrical torque in phase with the rotor angle by compensating the phase lag due to the transfer paths, *ICLOSE* and *TR*, as follows:

$$D_e = \frac{\Delta T_e}{\Delta \varpi_G} = (SODC)(ICLOSE)(TR) \tag{27}$$

$$SODC = \frac{D_e}{(ICLOSE)(TR)} \tag{28}$$

where D_e is a damping coefficient created by the SODC.

The input of the SODC is assumed to be rotor speed, but in practice it is convenient to use the generator real power (P_e) rather than rotor speed as the input signal. The rotor speed is vulnerable to mechanical noise, such as lateral vibration and tooth wear. Note that the real power lags rotor speed by 90 degrees. Therefore, the transfer function of the SODC can be modified in order to use generator real power, P_e, as an input signal as follows:

$$SODC = -\frac{D_e}{2H_g s(ICLOSE)(TR)} P_e \tag{29}$$

Using the NEA program, the frequency response analysis of the SODC can be performed while all of shaft inertia H is set to infinity so as to ignore the rotor inertia effects. If appropriate phase compensation of the SODC is made, eigenvalue analysis of the AC/DC system including shaft inertia effects is then used to determine the proper gain.

3.3 Time Domain Simulation: Step 3

As the last step, simultaneous off-line time domain simulation based on three-phase modeling of the power system is performed to verify the parameters of the SODC. Modeling of the HVDC system can be readily implemented using the EMTDC program, which has a power Graphic User Interface (GUI) environment for a PC. In the EMTDC, three-phase differential equation representation is used for transformers, lines, reactive compensation, harmonic filters, DC converters and other network elements. The switching of each individual thyristor is modeled on a cycle-by-cycle basis in this program.

3.4 The SODC Model and Its Input Signal

Fig. 6 indicates a block diagram of the SODC. A SODC consists of a transducer filter, washout filter, gain, two-stage phase compensation, and multi-order low pass filter. Two-stage washout filters are used to reduce the gain at

low frequencies. The gain, K, is determined by $K_a*T_w/2H$. A two-stage lead-lag block is used to compensate the phase lag due to the current controller and the transfer path, TR, represented in Fig. 5 above. Multi-stage low pass filters considerably reduce the effective gain at high frequencies. Linearization of the SODC's equations to be included in the NEA program is omitted in this paper.

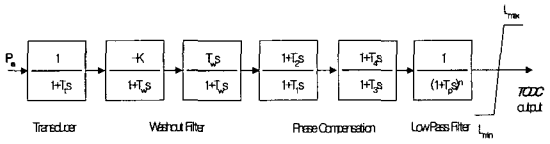

Fig. 6 Block Diagram of the SODC

Fig. 7(a) shows the calculated RMS generator real power using a Dynamic System Monitor (DSM) on a 620 MVA coal fired unit running at 3600 rpm. The DSM produces the phasor quantities of the measured voltages and currents by simultaneously sampling all inputs at a synchronous rate of four times the system frequency (240 Hz).

The result of discrete Fourier transform (DFT) analysis is displayed in Fig. 7(b). There are several modes involving lower frequency power oscillation modes and torsional modes as shown in Fig. 7(b). The dominant oscillation modes are power swing modes at less that 2 Hz. However, when a severe contingency occurs, the worst torsional mode may be stimulated. From such an analysis, we can be sure that the real generator power contains a torsional oscillation mode to some extent.

Fig. 8 depicts the natural frequencies and mode shapes of the rotor of an 892.4 MVA turbo-generator unit, which will be used in the SODC application for the AC/DC parallel transmission system described in this paper. Because we are considering a rotor with six masses, there are six modes of oscillation. The natural frequencies are 0.976 Hz, 15.74 Hz, 20.21 Hz, 25.55 Hz, 32.20 Hz, and 47.45 Hz.

The relative rotational displacements of the individual masses for each mode of oscillation are given by the right eigenvector of the corresponding eigenvalue. The 0.979 Hz mode represents the oscillation of the entire rotor against the power system. This is the mode normally considered in system stability studies. As seen by the mode shape, all six masses participate nearly equally in this mode. The other five modes represent the torsional modes of oscillation. The first torsional mode has a natural frequency of 15.74 Hz.

The generator rotor has very high relative amplitude of rotational displacement in the second torsional mode, 15.74 Hz, apart from the system mode, 0.976 Hz. This means that this mode can be easily excited by electrical torque supplied to the power system. Because electrical power is associated with the speed of the generator, use of electrical power as an input signal to the SODC is desirable.

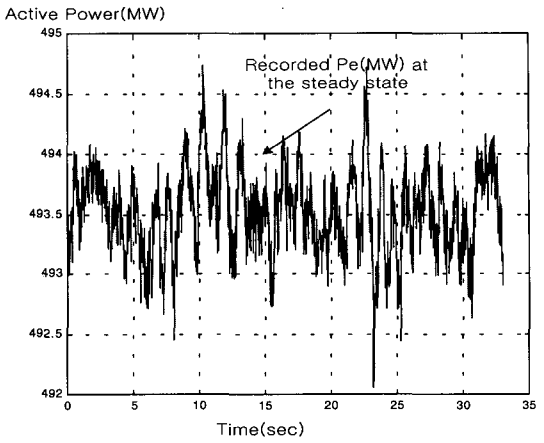

(a) Measured Generator Real Power at 620 MVA Coal Unit

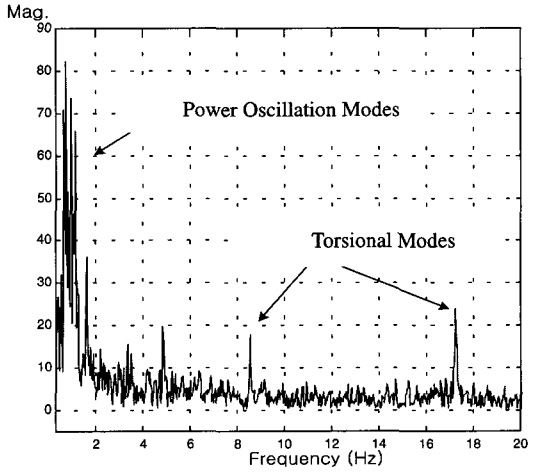

(b) Result of DFT of (a)

Fig. 7 Power Spectrum of Generator's Active Power

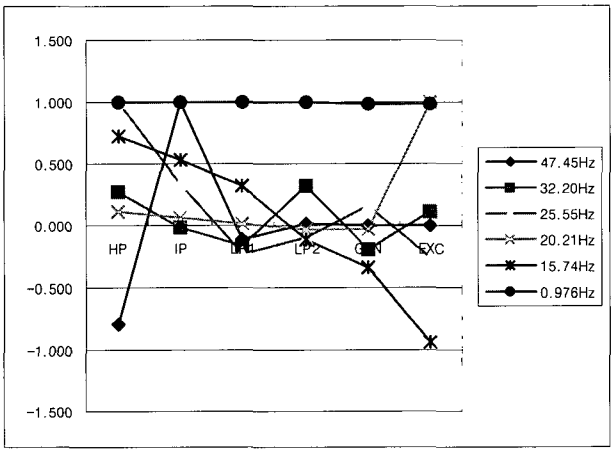

Fig. 8 Mode Shapes of 892.4 MVA Turbine-Generator Unit

4. Application of SODC to HVDC System

The suggested design method for the SODC is applied to two AC/DC systems. One AC/DC system has only a DC transmission line to transfer power, and the other has an

AC/DC parallel line to deliver the power. To model the shaft and machine, the machine and shaft parameters are taken from IEEE First Benchmark Model (FBM) [8], and for the DC system model the CIGRE HVDC Benchmark [30] is slightly modified. The simultaneous three-phase time-domain simulation uses the EMTDC [31] program.

4.1 Case 1: Single DC Transmission Line

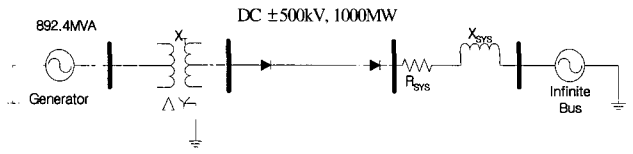

Fig. 9 A Radial Transmission Line with a DC Link

Fig. 9 shows one machine and a single DC transmission line connected to an infinite bus as an example for the design of the SODC. The worst operating condition for torsional oscillation in an AC/DC system is that a DC transmission line only is used to transmit the plant output. In this case, there is no positive electrical damping torque supplied by an AC transmission line. Note that mechanical damping is not considered in this study. This means that the mechanical damping is zero, $D_m = 0.0$.

4.1.1 Determination of the Dominant Torsional Mode

Using the NEA program, the characteristics of the AC/DC system including the machine, excitation system, torsional system, AC line, DC line, and control of the direct current is analyzed. In this eigenvalue analysis the static excitation system is assumed to control the terminal voltage of the machine, and any reactive compensation equipment and harmonic filters in the commutation bus are simply modeled as a single capacitor.

Table 1 shows the results of the eigenvalue analysis for different load conditions. There are five torsional modes and a single system mode. The more the load on the DC line is increased the more torsional modes become unstable. The worst torsional mode is at a frequency of 15.7 Hz. The real parts of eigenvalues represent the degree of damping; when those values are positive they indicate negative electrical damping. The system mode oscillates against the network without torsional vibration.

When most plant output is transmitted via a DC line, virtually zero synchronizing torque exists. The reason is that there is no synchronizing torque provided by an AC transmission line, although some is provided by the actions of the governor and excitation control. Because the synchronizing torque is very small, the frequency of the system mode oscillation is very low, as shown in Table 1.

The oscillation frequency of the system mode can be approximately predicted by $\omega_n = \sqrt{377K_1 / 2H}$, where K_1 is the synchronizing coefficient [16]. From the eigenvalue analysis above, the most critical frequency can be determined to be 15.7 Hz.

Table 1 Eigenvalues of Torsional Modes for Different Load Conditions

Mode	870 MW	600 MW	200 MW
	Eigenvalue	Eigenvalue	Eigenvalue
47.4 Hz	0.000 ±j 298.177	0.000 ±j 298.177	0.000 ±j 298.177
32.3 Hz	0.020 ±j 202.844	0.006 ±j 202.844	0.000 ±j 202.844
25.4 Hz	0.011 ±j 160.513	0.003 ±j 160.513	0.000 ±j 160.513
20.2 Hz	0.003 ±j 126.991	0.001 ±j 126.991	0.000 ±j 126.991
15.7 Hz	0.029 ±j 98.707	0.008 ±j 98.707	0.000 ±j 98.707
System Mode	3.064 ±j 1.837 (0.292 Hz)	2.400 ±j 1.125 (0.179 Hz)	–1.051 ±j 0.199 (0.032 Hz)

4.1.2 Phase Compensation of the SODC

The procedure for phase compensation assumes the generator rotor speed is the input signal. Then, the SODC is tuned to compensate for the phase lag due to the closed-loop current control, *ICLOSE*, and *TR* transfer function. Therefore, the SODC can produce electrical torque in phase with the rotor speed. As the final step, the input signal of the SODC is changed from rotor speed to electric power. The electric power lags rotor speed by 90 degrees; taking this phase lag into account, the phase compensation of the SODC is complete.

Fig. 10 shows the frequency response of the combined series transfer functions of the SODC and current regulator. In the Bode plot analysis the rotor speed is used as the input signal of the SODC and, instead of considering transfer function *TR* and *ICLOSE*, which includes a PI regulator and its closed-loop effect, the PI current regulator alone is considered. The response of the HVDC is so fast that the phase lag of the transfer path, *TR*, can be assumed to be negligible. The maximum gain is centered on 15 Hz and its phase lag is almost –360 degrees, which means compensation is complete, as shown in Fig. 10.

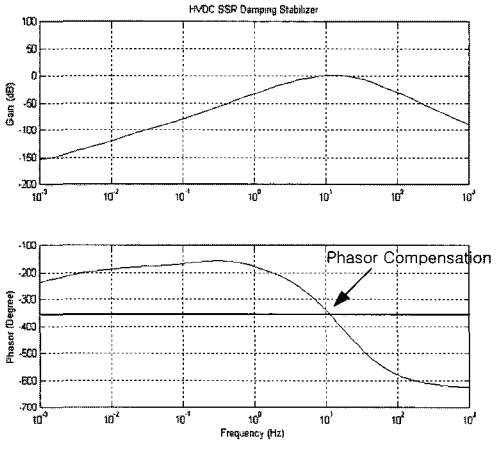

Fig. 10 Phase Compensation with Bode Plot

4.1.3 EMTDC Modeling

To run the simultaneous simulation, the AC/DC system described above was modeled using the EMTDC program. Fig. 11 indicates the graphic block diagram of the system, which has a multi-mass shaft system, a static excitation system, and a governor model with first-order valve systems.

Unlike the case in the eigenvalue analysis, governor action is considered to prevent simulation divergence because without governor control action it is impossible to run the time-domain simulation. Fig. 14 shows the block diagram of the governor model, Gov4, with $T_1 = 0.0$ and $T_2 = 0.04$ seconds time constant and valve model, which is modeled as a first order with T = 2.0 seconds and a gain of G = 1.

Fig. 13 indicates the PI current regulator and the SODC on the rectifier side. The gains of the PI regulator are $K_I = 0.01$ and $K_P = 1.0$. To construct the 12–pulse bridge converter the build-in thyristor model in EMTDC was used. The DC line is modeled as a T circuit, and the values of reactance, resistance, and capacitance are 0.5968 H, 2.5 Ω, and 26 uF, respectively. The HVDC bipole system is modeled with PSCAD/EMTDC.

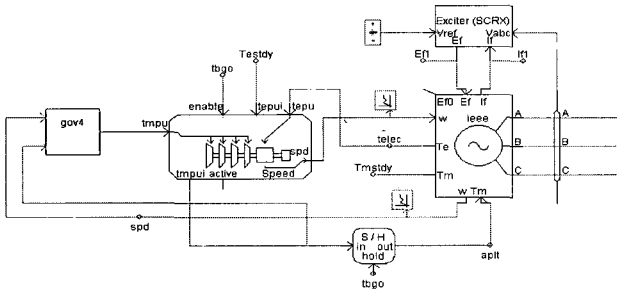

Fig. 11 Generation System with Excitation and Governor System

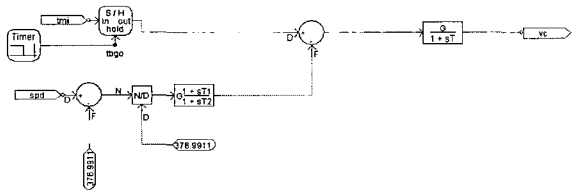

Fig. 12 Governor and Valve Modeling of Gov4

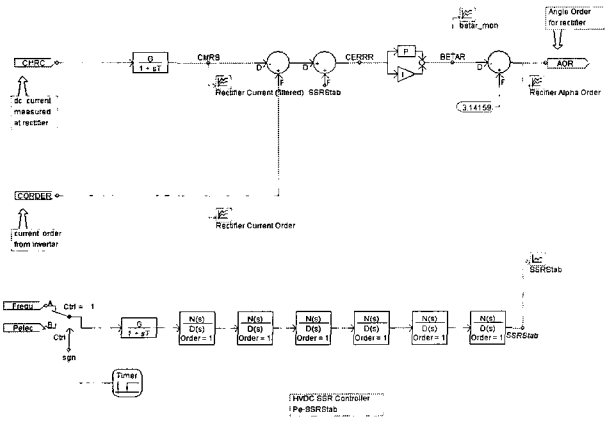

Fig. 13 PI Controller and Damping Controller on the Rectifier Side

4.1.4 Time-Domain Simulation

The three-phase simultaneous time domain simulation program, EMTDC, was used to verify the design procedure of the SODC. The operating condition in the steady state is assumed to be the 870 MW that the DC line is carrying. This system is inherently unstable with respect to small signal stability due to the PI controller in the rectifier, even without contingency. This system, in which only one generator is supplying an isolated DC load, contains considerable nonlinear characteristics due to the governor having a speed-droop characteristic. The time-domain simulation showed that frequency deviated slightly from the fundamental frequency (60 Hz) because of an imbalance between generation and load. The used integral time step is 50 microseconds.

■ Without Damping Controller

Fig. 14 presents the response, after initialization of 1.499 seconds, of rotor speed without the SODC. The oscillation in the machine speed explicitly illustrates the system mode, which has a low frequency of approximately 0.1 Hz. The low frequency of oscillation is due to the lack of synchronizing torque but the positive damping of the system mode is provided by the fast response governor. The control of the governor is deliberately designed to maintain positive damping on the system mode so that the stability of the torsional oscillation can be observed. With no fast governor control the speed response will diverge. Fig. 15 shows the instability of the torsional oscillation in LPA-LPB at 15.7 Hz, which is the most unstable mode of the torsional modes. In this simulation, the mechanical damping coefficient is not considered, so most of the negative damping contribution is a result of the electrical system. Further responses of the remaining torsional modes machine responses, HVDC response, and controller responses are given in Appendix D.

■ With Damping Controller

Fig. 16 illustrates the response of machine rotor speed with the SODC. There is little improvement in the damping of the system mode due to the SODC, although the SODC is designed to damp the torsional oscillation near 15.0 Hz. However, the frequency of the system mode was not changed significantly. The gain of the SODC was tuned to K = –0.60; Fig. 17 illustrates the improved damping of the torsional oscillation. Surprisingly the eigenvalue analysis including the SODC did not indicate any variation of the torsional modes even with larger gain. It is conjectured that this is due to the nonlinear characteristics of the one

machine and one load system. The governor with speed-droop characteristics used in this system causes the frequency of the system to deviate from the fundamental frequency, 60 Hz. However, the state equations are derived on the basis of this fundamental frequency.

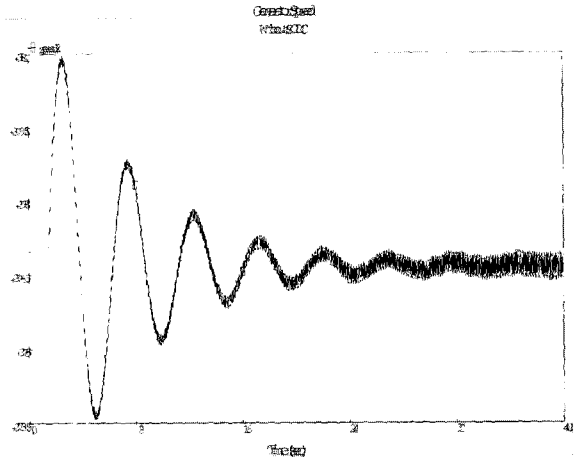

Fig. 14 Generator Rotor Speed (without SODC)

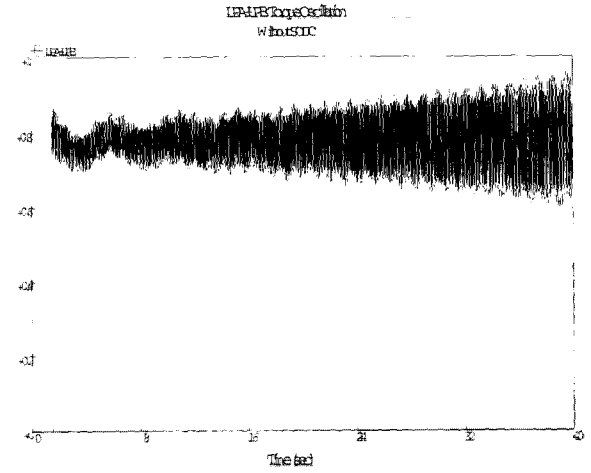

Fig. 15 LPA-LPB Torque Response (without SODC)

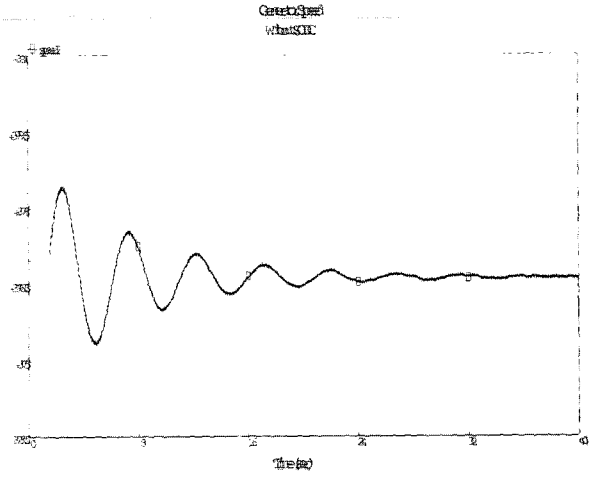

Fig. 16 Generator Rotor Speed (with SODC)

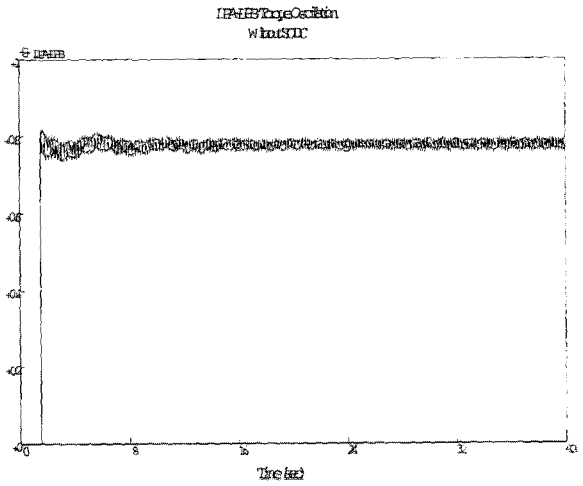

Fig. 17 LPA-LPB Torque Response (with SODC)

4.2 Case 2: AC/DC Parallel Transmission

In this section, a HVDC system in parallel with an AC line is considered. The system modeling is the same as for the previous case except that an AC line is included. Fig. 18 shows the DC line in parallel with the AC line. This system is so unstable that no incident is required to cause oscillation of the torsional modes in the simultaneous time-domain simulation.

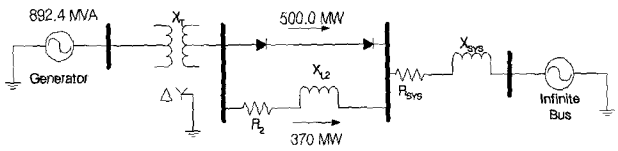

Fig. 18 DC Line in Parallel with AC Line

4.2.1 Determination of the Dominant Torsional Mode

Table 2 indicates the eigenvalues of the AC/DC system for different loads with a static excitation system but no governor model. If a governor model, Gov4, with T = 2.0 sec is used the damping ratio is improved slightly, less than 0.4%. As DC loading is increased the real parts of the eigenvalues become larger positive values. The inclusion of the AC transmission line affects the frequency of system mode.

Table 2 Eigenvalues of Torsional Modes for Different Loads

Mode	870 MW DC 0.0 MW AC	500 MW DC 370 MW AC	300 MW DC 570 MW AC
	Eigenvalue	Eigenvalue	Eigenvalue
47.4 Hz	0.000 ±j 298.177	0.000 ±j 298.177	0.000 ±j 298.177
32.3 Hz	0.030 ±j 202.844	0.014 ±j 202.844	0.009 ±j 202.844
25.4 Hz	0.015 ±j 160.513	0.007 ±j 160.513	0.005 ±j 160.513
20.2 Hz	0.004 ±j 126.991	0.002 ±j 126.991	0.001 ±j 126.991
15.7 Hz	0.035 ±j 98.707	0.018 ±j 98.707	0.010 ±j 98.707
System Mode	1.427 ±j 5.309 (0.845 Hz)	0.929 ±j 6.141 (0.977 Hz)	0.738 ±j 6.256 (0.996 Hz)

4.2.2 Design of Phase Compensation

The phase compensation of the SODC is shown in Fig. 19. The maximum gain shown in Fig. 19 is in the frequency range 15.7 Hz to 20.0 Hz. Therefore, the system mode below 2 Hz is not affected by the SODC. In this phase compensation, low pass filters of order 4 are used to filter out frequencies higher than 15 Hz so as not to provide negative damping torque for the remaining torsional modes due to phasor lag in the system. Although the SODC is designed to provide positive torque for the lowest torsional mode (15 Hz), some torsional modes near 15 Hz may be affected, so the phase compensation should be adjusted to provide additional damping torque for those modes.

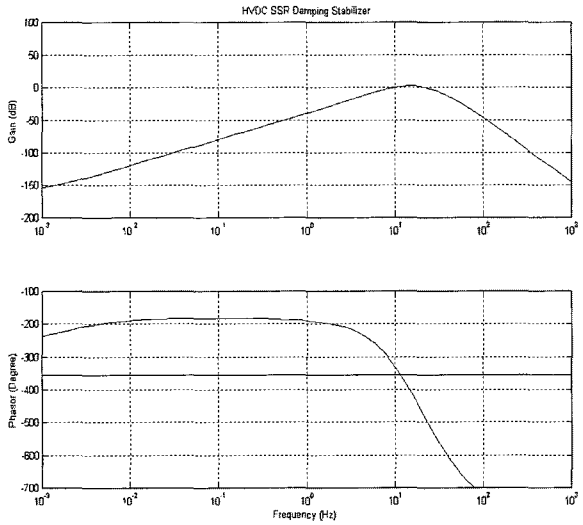

Fig. 19 Phase Compensation with Bode Plot

4.2.3 Time-Domain Simulation

In the EMTDC time domain simulation, torsional modes are observed only in the steady-state conditions. Because the DC link with a parallel AC transmission line is so unstable, it indicates undamped torsional oscillations without any perturbations. After initializing the network states and machine states, the torsional systems are released after 1.499 seconds for simulation together with the other systems in the EMTDC simulation. 500 MW is transmitted using the DC link, and the remaining power is transmitted via the AC line. To provide the electrical damping torque for a system mode below 2 Hz, the time constant of the turbine valve was set to 1.0 second. The effects of the governor and valve action on the torsional modes are negligible due to the system's slow dynamics.

■ Without Damping Controller

Fig. 20 depicts the rotor angle response when the network and machine states are initialized and the turbine systems are then released without the SODC. At first the system mode appears in the rotor angle oscillations; then the undamped torsional oscillation of the system mode becomes larger. Fig. 21 shows the torsional oscillation of the LPA-LPB shaft torque without the SODC. It also represents only the negative electrical damping caused by the DC links and AC line because the mechanical damping component is not considered in this time-domain simulation.

■ With Damping Controller

Figs. 22 and 23 show the response of rotor angle and LPA-LPB shaft torque with the SODC. In contrast to previous results without the SODC, the torsional oscillations are to some extent damped. Therefore, the SODC can compensate the negative electrical damping caused by the electrical system, such as DC links and AC lines. If the mechanical self-damping effects are considered greater damping of the torsional oscillation can be obtained The gain of the SODC is tuned as K = –0.60, giving some margin to the critical damping torque. This means that slightly increasing the gain of the SODC can provide further torsional damping torque.

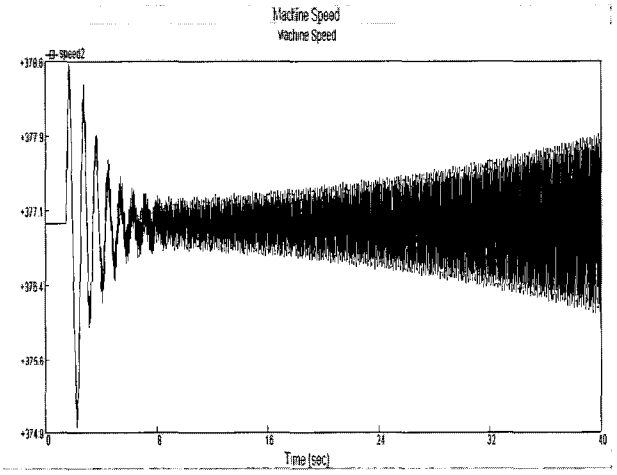

Fig. 20 Generator Rotor Speed without SODC

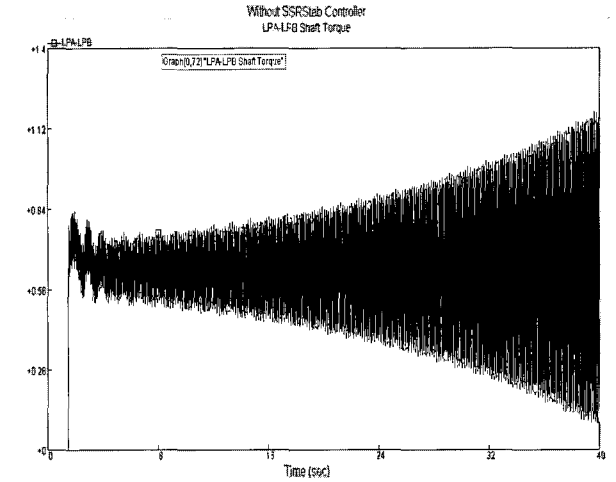

Fig. 21 Torsional Oscillation Response without SODC (LPA-LPB)

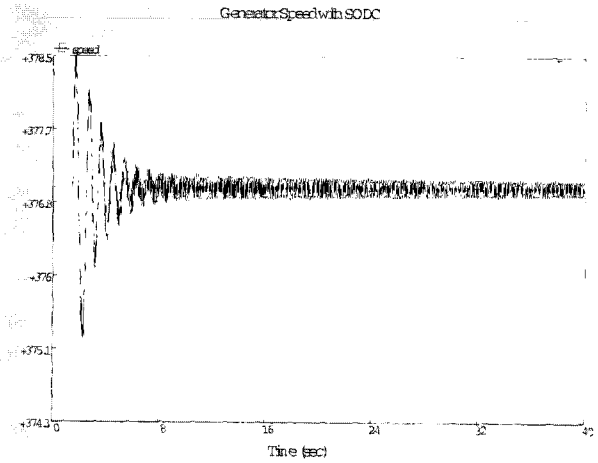

Fig. 22 Generator Rotor Speed with SODC

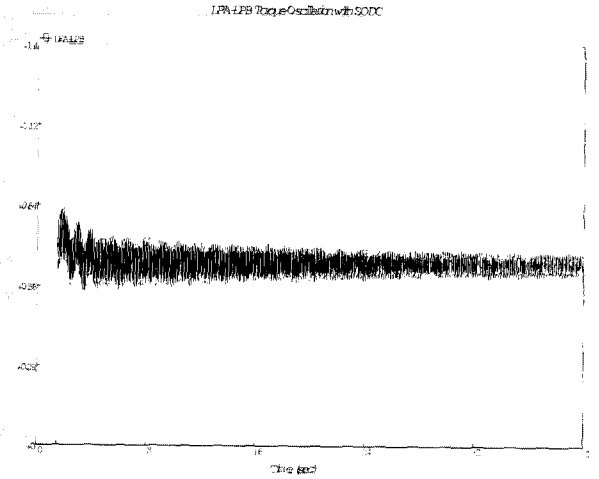

Fig. 23 Torsional Oscillation Response with SODC (LPA-LPB)

It is important to determine the optimal gain by considering the gain margin of the SODC, which can be determined between the chosen gain and the maximum gain in which unstable oscillations may occur. However, the gain margin depends on the given system, and many eigenvalue studies and simultaneous time-domain simulations are required to verify the gain of the SODC. Because determining the optimal gain of the SODC by considering the gain margin is beyond the scope of this paper, explanation of gain optimization will be omitted.

4.2.4 Results of the Eigenvalue Analysis

Table 3 depicts the results of the eigenvalue analysis of the AC/DC system with the SODC. This system is a more practical system than that of Case 1. The designed SODC parameters enhance the degree of stability of most of the torsional modes. Although the 15.76 Hz is the main target mode for which the SODC is supposed to provide positive damping torque, the remaining modes are also provided with some positive damping torque.

In this eigenvalue study, the per unit values of the proportional gain (K_P) and integral gain (K_I) in the PI controller in the HVDC system are assumed to be 15.0 per unit and 1.5 per unit instead of 1.0 and 0.01, respectively. The values of the PI gains in the CIGRE Benchmark system are provided with engineering values; therefore, these PI gains should be converted to per unit values, but it is difficult to compute the accurate comprehensive PI gains including the hidden gain in the bridge. Therefore, the values of PI gains per unit used are referred to [7].

Table 3 Eigenvalues of Torsional Modes with SODC

Mode	500 MW DC, 370 MW AC	
	Eigenvalue	Frequency
Torsional Modes	0.000 ±j 298.177	47.456 Hz
	0.008 ±j 202.844	32.301 Hz
	0.003 ±j 160.513	25.559 Hz
	-0.001 ±j 127.015	20.215 Hz
	-0.016 ±j 99.020	15.760 Hz

5. Conclusion

This paper describes a new approach to HVDC system control for damping subsynchronous oscillation in the HVDC system and the turbine generator shaft systems. The main contributions of this paper can be summarized as follows:

■ The suggested SODC design method consists of three steps; the first step is to determine the worst torsional mode of several torsional modes using the NEA program. Then, the parameters of the supplementary damping controller are designed for the frequency range of the torsional mode determined using the frequency response of the SODC and HVDC current controller at the rectifier. Finally, an off-line simultaneous three-phase time domain simulation program is used to verify the parameters of the controller.

■ The suggested SODC uses adjacent generator active power (P_e) because the generator active power is free from mechanical noise such as lateral vibration or tooth wear. In addition, it contains torsional information with proper magnitude so that the phasor compensation and gain tuning of the SODC parameters can be made with ease. The performance of the SODC can be enhanced more if the SODC is realized by taking advantage of state-of-art digital signal processing technology.

■ The practicality of the suggested SODC design procedure for damping torsional modes in the combined AC/DC system has been verified by application, using the PSCAD/EMTDC program, to two combined AC/DC systems that have inherently unstable torsional modes.

For improved application of the suggested SODC, more research is required on the following topic. The reactive power supplied by the generator and a reactive compensator near the HVDC converter station may play an

important role in determining the stability of the torsional modes. Therefore, further studies are required, both on the voltage control by the generator and on the degree of compensation of the reactive power supplied by a capacitor that is installed for compensating the reactive power consumed by the HVDC system.

Acknowledgements

This work was sponsored by the Advanced Power System Research Center at Korea University, and supported by the Ministry of Commerce, Industry and Energy in Korea.

Appendix

A. Rectifier Dynamic Equations:

$$V_{dcr} = N_i\left(\frac{3\sqrt{2}}{\pi} E_{acr}\cos\alpha - \frac{3X_{ci}I_{dcr}}{\pi} - L_{ci}\frac{dI_{dcr}}{dt} - 2R_{ci}I_{dcr}\right) \quad (A.1)$$

$$L_{dc}\frac{dI_{dcr}}{dt} = V_{dcr} - I_{dcr}R_{dc} - V_{dcl} \quad (A.21)$$

B. Inverter Dynamic Equations:

$$V_{dci} = N_i\left(\frac{3\sqrt{2}}{\pi} E_{aci}\cos\gamma - \frac{3X_{ci}I_{dci}}{\pi} - L_{ci}\frac{dI_{dci}}{dt} + 2R_{ci}I_{dci}\right) \quad (A.3)$$

$$L_{dc}\frac{dI_{dci}}{dt} = V_{dcl} - V_{dci} \quad (A.4)$$

C. DC Line Dynamic Equations:

$$C_{dcl}\frac{dV_{dcl}}{dt} = I_{dcr} - I_{dcl} \quad (A.5)$$

References

[1] Bahrman,m., Larsen.E.V., Piwko.R.W., and Patel. H.S.: "Experience with HVDC-turbine-generator torsional interaction at square butte", IEEE Trans., 1980. PAS-99, (5), pp.966-976

[2] IEEE SSR Working Group, "Proposed Terms and Definitions for Subsynchronous Resonance," IEEE Symposium on Countermeasures for Subsynchronous Resonance, IEEE Pub, 81TH0086-9-PWR, 1981, p92-97

[3] IEEE SSR Working Group, "Terms, Definitions and Symbols for Subsynchronous Oscillations", IEEE Trans., PAS-104, No. 6, June 1985

[4] R.J.Piwko, E.V.Larsen, HVDC System Control for Damping of Subsynchronous Oscillations, EL-2708, EPRI, 1982

[5] M. Takasaki, "Study of AC/DC Power System Dynamic Instability and its Control", CRIEPI, T23.

[6] Kundur.P, Rogers, G.J., Wang, D.Y., and Lauby, M.G., "A comprehensive computer program package for small signal stability analysis of power systems', IEEE Trans., VPWRS-5, (4), pp.1076-1086, 1990

[7] Arabi, Rogers, G.J., Wang.D.Y, and Kundur.P, "Small signal stability program analysis of SVC and HVDC in power systems', IEEE Trans., 1991, PWRS-6(3), pp. 1147-1153

[8] IEEE SSR Working Group, "First benchmark model for computer simulation of subsynchronous resonance" , IEEE Trans., Vol. PAS-96, September/October 1977

[9] IEEE SSR Working Group, "Second benchmark model for computer simulation of subsynchronous resonance" , IEEE Trans., Vol. PAS-104, 1985

[10] M.Parniani, M.R.Iravani, "Computer anlaysis of small-signal stability of power systems including network dynamics", IEE Proc-Gener. Transm. Distrib Vol.142, No. 6, Novemver 1995

[11] E.V. LARSEN and PRICE.W.W., "MANSTAB/ POSSIM power system dynamic analysis programs- a new approach combining nonlinear simulation and linearized state-space/frequency domain capabilities', IEEE PICA Proceedings, 1977, pp.350-359

[12] M.R.Iravani, "A software tool for coordination of controllers in power systems", IEEE, Trans. On Power Systems, Vol. 5, No-1, February 1990

[13] KUH.E.S., and Rohrer.R.A., "The state variable approach to network analysis", Proc., IEEE, 1965, pp.672-686

[14] Visual Numerics, IMSL Math/Library User/s Manual Vol.1, 2000.

[15] Manitoba HVDC Research Centre, PSCAD/EMTDC power systems simulation software tutorial manual, 1994

[16] F.P. DeMello, C.Concordia, "Concepts of Synchronous Machine Stability as Affected by Excitation Control", IEEE Trans., vol.PAS-88, No. 4, pp.316-329, Apr. 1969

[17] P.M.Anderson, B.L.Agrawal, J.E.Van Ness, Subsynchronous Resonance in Power Systems, IEEE Press 1990, pp 233

[18] P.Kundur, Power System Stability and Control, McGraw-Hill, 1994

[19] W. Shi, M. R. Iravani, "Effect of HVDC Line Faults on Transient Torsional Torques of Turbine Generator Shafts", IEEE Transaction, Vol. PWRS-9, No.3,

August 1994
[20] A. H. Rahim, I. M. Amin, "Stabilization of a High Voltage ACDC Power System", IEEE Transaction, Vol. PAS-104, No. 11, November 1985
[21] D. J. Kim, H. K. Nam, Y. H. Moon, "A Novel Analysis Program of Small-Signal Stability of Power System Including Network Dynamics", ICEE 2002, Jeju.
[22] D.J.Kim, H.K.Nam, Y.H.Moon, "Universal SSR Small Signal Stability Analysis Program of Power Systems and its Applications to IEEE Benchmark Systems", KIEE, No.3 September 2003.
[23] E. V. Larsen, D. A. Swann, "Applying Power System Stabilizers, Part I, II, and III", IEEE Transaction, Vol. PAS-100, No.6, June, 1981, pp.3017-3046
[24] D.J.Kim, Y.H.Moon, Jin.Hur, J.H.Shin, T.K.Kim, J.B.Choo "A Practical Tuning Method of Dual-Input PSS and its Application to Large Power System" Trans. KIEE. Vol.51A, No.7, July 2002
[25] B. K. Johnson, F. P. de Mello, J. M. Undrill, "Comparing Fundamental Frequency and Differential Equation Representation of AC/DC", IEEE Transaction, Vol. PAS-101, No. 9, Sep. 1982.
[26] E. W. Kimbark, Direct Current Transmission, Vol. I, 1971, John Wiley and Sons, Inc., USA.
[27] R. Jotten, J. P. Bowles, G. Liss, C. J. B. Martin and E. Rumpf," Control in HVDC Systems, The State of the Art, Part I: Two Terminal Systems," CIGRE Paper 14-10, 1978
[28] G. K. Carter, C. E. Grund, H. H. Happ, R. V. Pohl, "The Dynamics of AC/DC Systems with Controlled Multi-terminal HVDC Transmission", IEEE Transaction, Vol. PAS-96, No.2, March/April 1977
[29] A. Ekstrom, G. Liss, "A Refined HVDC Control System" IEEE Transaction, Vol. PAS-89 May/June 1970 pp 723-732
[30] CIGRE WG 14-02: "First Benchmark Model for HVDC Control Studies", Electa, April 1991, (135), pp. 55-75
[31] PSCAD/EMTDC ver 3.0.8, 2002.

Dong-Joon Kim
He received his B.S., M.S. and Ph.D. degrees in Electrical Engineering from Chonnam National University, Korea, in 1992, 1994, and 2004, respectively. He has been with KERI since 1994 and is now a Senior Research Engineer. His interests include analysis of voltage stability, dynamic modeling of power plants, control of HVDC modeling, and application of digital PSS. He is a Member of KIEE and IEEE.

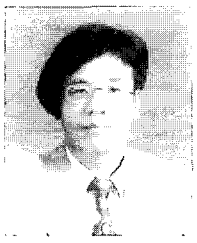

Hae-Kon Nam
He received his B.S. degree from Seoul National University, Korea, in 1975, his M.S. degree from the University of Houston, Houston, Texas, in 1980, and his Ph.D. degree from the University of Texas, Austin, Texas, in 1986, all in Electrical Engineering. From 1986 to 1988, he worked as a Senior Research Engineer at KERI. Since 1988 he has been with Chonnam National University where he is now a Professor of Electrical Engineering. He was also a Visiting Professor at Pennsylvania State University and Powertech Labs Inc. in 1994 and 2001, respectively. His interests include power system stability and power plant modeling and control. He is a Member of KIEE and IEEE.

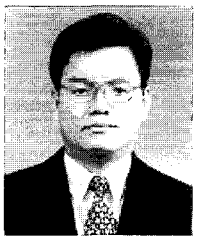

Young-Hwan Moon
He received his B.S. and M.S. degrees from Seoul National University, Korea, in 1979 and 1981, respectively, and his Ph.D. from the University of Texas, Arlington in 1990, all in Electrical Engineering. He has been with KERI since 1981 and is now a Principal Research Engineer. His interests include modeling of power systems, application of digital PSS, design of electricity markets and control of HVDC transmission. He is a member of KIEE. IEEE and Tau Beta Pi.